Research Article

Raymundus Lullus Lambang Govinda Hidayat, Wibowo, Budi Santoso, Fitrian Imaddudin and Ubaidillah*

Selection of MR damper model suitable for SMC applied to semi-active suspension system by using similarity measures

https://doi.org/10.1515/eng-2022-0367
received July 17, 2021; accepted August 05, 2022

Abstract: This article discusses the research to determine the suitable magnetorheological (MR) damper model to produce the damping force generated by the sliding mode control (SMC) strategy. The MR damper models studied are parametric, i.e., the Bingham model, the Bouc-Wen model, and the Bouc-Wen model with a hyperbolic tangent function. The damping force of SMC usually includes sudden changes in the force and chattering. The research was carried out by calculating the value of the similarity measure of the damping force of the controller and the damping force of each model. The results show that the two Bouc Wen models had a high similarity measure. The Bouc Wen model with the hyperbolic tangent function was selected because it provides a sudden change of force and reasonable force tracking needed to develop the inverse MR damper model.

Keywords: damping force, magnetorheological device, semi-active suspension system, sliding mode control

1 Introduction

Rheological devices have recently become an intensive research theme as well as their application in the field of vibration control and isolators (structural dampers for earthquakes [1], vehicle suspensions [2–6], and seat suspensions [7–9]). However, to be applied effectively, properties of advanced material, the modeling of the magnetorheological (MR) devices, and the control strategy have to be appropriately selected.

The sliding mode controller (SMC) strategy selects a sliding surface and switching actions to bring the control variables to an initial state or reference condition within a particular time. The choice of the sliding surface is based on the sliding function. When the states are on a sliding surface, the states are forced to remain on the sliding surface. Switching actions work on the state variables and control them so that they are around the sliding surface and go to the origin within a particular time.

Researches on implementing SMC are presented in refs. [2–5]. Previous studies [2,3] apply the SMC strategy to the MR damper as a component of a semi-active suspension system. In previous studies [4,5], the MR damper is applied in an active suspension system, while in ref. [6], the control strategy used is the PID controller. This study chose SMC for the suspension controller system because it is suspected that SMC can respond to inputs or disturbances that change suddenly, such as disturbances that occur in vehicles on the highway. SMC can also generate nonlinear forces that match the nonlinear forces generated by the MR damper.

In SMC, control action consists of equivalent action and switching action. Switching action is a discontinuous function, i.e., a signum function that leads to chattering. Chattering is a phenomenon where the controlled state variables oscillate around a sliding surface. Therefore, implementing an SMC strategy that uses the MR damper has to consider the MR damper specifications and the chattering phenomenon.

Furthermore, this study chose an MR damper model that can produce damping force from this SMC controller. The study compared the Bingham model [10], the Bouc Wen model [10], and the Bouc Wen model with a hyperbolic tangent [11]. The current research was carried out by comparing the value of the similarity measure between

* **Corresponding author: Ubaidillah,** Mechanical Engineering Department, Faculty of Engineering, Universitas Sebelas Maret, Surakarta, Indonesia, e-mail: ubaidillah_ft@staff.uns.ac.id
Raymundus Lullus Lambang Govinda Hidayat: Mechanical Engineering Department, Faculty of Engineering, Universitas Sebelas Maret, Surakarta, Indonesia, e-mail: lulus_l@staff.uns.ac.id
Wibowo, Budi Santoso, Fitrian Imaddudin: Mechanical Engineering Department, Faculty of Engineering, Universitas Sebelas Maret, Surakarta, Indonesia

the damping force of the controller and the damping force of each model. A similarity measure measures the similarity of the damping force of the controller and the damping force of the MR damper model so that a functional product design can be obtained.

The research objective is to obtain an MR damper model that can produce commanded damping force from an SMC controller. The selected MR damper model must be simple, consider the ease of obtaining an inverse model, and be implemented with hardware.

The rest of this article is organized as follows. This research is computer simulation research. Section 2 discusses the simulation setup. Section 3 describes the results and discussion and includes benchmarking with previous studies. Finally, the conclusions are presented in Section 4.

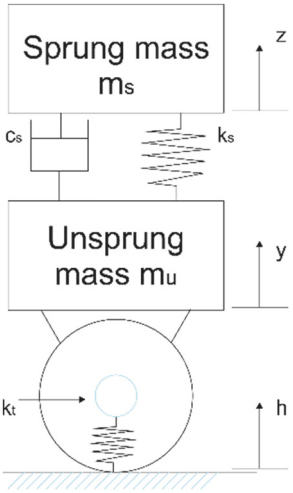

Figure 1: Quartenion car model [12].

2 Simulation setup

This study is a simulation to investigate the performance of a semi-active suspension system that implements the SMC strategy. The suspension system was chosen because the objective is to reduce vibration due to the road roughness profile transmitted to the vehicle body. Furthermore, the suspension system should provide ride comfort and good handling [2]. However, these objectives are contradictory; ride comfort requires soft suspension (soft springs), while good handling is achieved by rigid suspension (stiff springs). Therefore, designing a controller that meets these objectives is an exciting and challenging task. First, the model of the quarter car model of suspension as shown in Figure 1 [12] is used, and then the equations of motion (1) and (2) are obtained:

$$m_s\ddot{z} = -c_s(\dot{z} - \dot{y}) - k_s(z - y), \tag{1}$$

$$m_u\ddot{y} = -c_s(\dot{y} - \dot{z}) - k_s(y - z) - k_t(y - h), \tag{2}$$

m_s is sprung mass; m_u is unsprung mass; c_s is suspension damping coefficient; k_s is suspension springs constant; and k_t is tyre spring constants. y and $\dot{y}$ are unsprung mass displacement and velocity, respectively. z and $\dot{z}$ are sprung mass displacement and velocity, respectively.

3 SEMI-active suspension system

The semi-active suspension system is obtained by adding a semi-active damping element between the sprung mass and unsprung mass in the quarter car model as shown in Figure 1. The semi-active damping force is expressed by f_d. Furthermore, the semi-active suspension system is expressed as a state space equation as shown in equation (3), $x_1 = z$, $x_2 = y$ and $x_3 = \dot{x}_1$; $x_4 = \dot{x}_2$. The semi-active suspension equations of motion are as follows:

$$\begin{aligned}
\dot{x}_1 &= x_3,\\
\dot{x}_2 &= x_4,\\
\dot{x}_3 &= -\frac{c_s}{m_s}(x_3 - x_4) - \frac{k_s}{m_s}(x_1 - x_2) - \frac{1}{m_s}f_d,\\
\dot{x}_4 &= -\frac{c_s}{m_u}(x_4 - x_3) - \frac{k_s}{m_u}(x_2 - x_1) - \frac{k_t}{m_u}(x_2 - h)\\
&\quad + \frac{1}{m_u}f_d,
\end{aligned} \tag{3}$$

where f_d is a damping force. Suspension deflection is determined as follows: $y : y = x_1 - x_2$, i.e., sprung mass deflection minus unsprung mass deflection.

4 SMC for suspension system

The objective of the suspension control system is to make suspension deflection y fast and accurately follows the set point, y_d. Suspension system tracking error e is determined as follows in equations (4)–(9):

$$e = y_d - y, \tag{4}$$

The sliding surface is

$$s = \dot{e} + ce, \tag{5}$$

where c is a positive constant. Derivative of sliding surface with respect to time is:

$$\dot{s} = \ddot{e} + c\dot{e}, \tag{6}$$

where $\dot{e}$ is

$$\dot{e} = \dot{y}_d - \dot{y} = \dot{y}_d - (\dot{x}_1 - \dot{x}_2) = \dot{y}_d - (x_3 - x_4), \tag{7}$$

and $\ddot{e}$ is

$$\begin{aligned}\ddot{e} &= \ddot{y}_d - (\dot{x}_3 - \dot{x}_4) = \ddot{y}_d - \dot{x}_3 + \dot{x}_4 \\ &= \ddot{y}_d + \frac{c_s}{m_s}(x_3 - x_4) + \frac{k_s}{m_s}(x_1 - x_2) + \frac{1}{m_s}f_d \\ &\quad - \frac{c_s}{m_u}(x_4 - x_3) - \frac{k_s}{m_u}(x_2 - x_1) - \frac{k_t}{m_u}(x_2 - h) + \frac{1}{m_u}f_d \\ &= \ddot{y}_d + \left(\frac{k_s}{m_s} + \frac{k_s}{m_u}\right)x_1 + \left(-\frac{k_s}{m_s} - \frac{k_s}{m_u} - \frac{k_t}{m_u}\right)x_2 \\ &\quad + \left(\frac{c_s}{m_s} + \frac{c_s}{m_u}\right)x_3 + \left(-\frac{c_s}{m_s} - \frac{c_s}{m_u}\right)x_4 + \frac{k_t}{m_u}h \\ &\quad + \left(\frac{1}{m_s} + \frac{1}{m_u}\right)f_d.\end{aligned} \tag{8}$$

Therefore,

$$\begin{aligned}\dot{s} &= c\dot{e} + \ddot{e} \\ &= c(\dot{y}_d - x_3 + x_4) + \ddot{y}_d + \left(\frac{k_s}{m_s} + \frac{k_s}{m_u}\right)x_1 \\ &\quad + \left(-\frac{k_s}{m_s} - \frac{k_s}{m_u} - \frac{k_t}{m_u}\right)x_2 \\ &\quad + \left(\frac{c_s}{m_s} + \frac{c_s}{m_u}\right)x_3 + \left(-\frac{c_s}{m_s} - \frac{c_s}{m_u}\right)x_4 + \frac{k_t}{m_u}h \\ &\quad + \left(\frac{1}{m_s} + \frac{1}{m_u}\right)f_d.\end{aligned} \tag{9}$$

SMC consists of the reaching phase and the sliding phase. The reaching phase is when state variables move to a stable manifold and stay in the sliding phase, and the state variables are moved to the equilibrium point by a reaching law. In this research, the reaching law equation (10) is determined as follows:

$$\dot{s} = -\epsilon\ \mathrm{sign}(s) - ks,\ \epsilon > 0,\ k > 0. \tag{10}$$

By equating the two previous equations, damping force is obtained as shown in equation (11):

$$\begin{aligned}f_d &= (m_s m_u)/(m_s + m_u)[-\epsilon\ \mathrm{sign}\,(s) - ks - c(\dot{y}_d - x_3 + x_4) - \ddot{y}_d \\ &\quad - \left(\frac{k_s}{m_s} + \frac{k_s}{m_u}\right)x_1 - \left(-\frac{k_s}{m_s} - \frac{k_s}{m_u} - \frac{k_t}{m_u}\right)x_2 - \left(\frac{c_s}{m_s} + \frac{c_s}{m_u}\right)x_3 \\ &\quad - \left(-\frac{c_s}{m_s} - \frac{c_s}{m_u}\right)x_4 - \frac{k_t}{m_u}h\Bigg].\end{aligned} \tag{11}$$

Damping force is equivalent to SMC signal u and consists of an equivalent control u_{eq} and a switching control signal u_{sw}, which are sequentially written in equations (12)–(14):

$$u = u_{eq} + u_{sw}, \tag{12}$$

where

$$\begin{aligned}u_{eq} &= (m_s m_u)/(m_s + m_u)\Bigg[-c(\dot{y}_d - x_3 + x_4) - \ddot{y}_d - \left(\frac{k_s}{m_s} + \frac{k_s}{m_u}\right)x_1 \\ &\quad - \left(-\frac{k_s}{m_s} - \frac{k_s}{m_u} - \frac{k_t}{m_u}\right)x_2 - \left(\frac{c_s}{m_s} + \frac{c_s}{m_u}\right)x_3 \\ &\quad - \left(-\frac{c_s}{m_s} - \frac{c_s}{m_u}\right)x_4 - \frac{k_t}{m_u}h\Bigg],\end{aligned} \tag{13}$$

and

$$u_{sw} = -\frac{m_s m_u}{m_s + m_u}[\epsilon\ \mathrm{sign}(s) + ks]. \tag{14}$$

5 The selection of MR damper model

MR damper is expected to work better than ER damper in several ways, i.e., operation temperature range, maximum yield stress, and sensitivity to impurities [13]. In addition, the performance of the MR damper is not sensitive to temperature change because the magnetic polarization mechanism remains unchanged in the operating temperature range.

As a semi-active element in a control system, a realistic MR damper model is desirable to analyze control system performance. Therefore, the MR damper model has to be simple as possible and able to simulate the nonlinear property of the MR damper so that it can be effectively applied with a control algorithm. Models that are widely used are the Bingham model and Bouc-Wen model, as shown in Figure 2.

The Bingham model and the Bouc-Wen model are parametric dampers MR models. The damping force is expressed by equations (15) and (16):

$$\text{Bingham model: } F_{Bh} = F_0 + c_v\dot{x} + F_y\mathrm{sign}(\dot{x}), \tag{15}$$

$$\text{Bouc} - \text{Wen model: } F = c_0\dot{x} + k_0(x - x_0) + \alpha z. \tag{16}$$

The variable $\dot{z}$ determines the velocity–force nonlinear hysteresis property of the MR damper as follows [10]:

$$\dot{z} = -\gamma z|\dot{x}||z|^{n-1} - \beta\dot{x}|z|^n + A\dot{x}. \tag{17}$$

z is also determined by using the hyperbolic tangent function [11] as follows:

$$z = \tanh(\beta\dot{x} + \delta\ \mathrm{sign}(x)). \tag{18}$$

In this research, initial values are $x_0 = 0$ [13]. Both α and c_0 parameters depend on voltage input, V supplied to the damper. The α parameter is calculated as follows [10]:

$$\alpha(V) = 2.3363\ \times V^2 - 3.4209 \times V + 5{,}000. \tag{19}$$

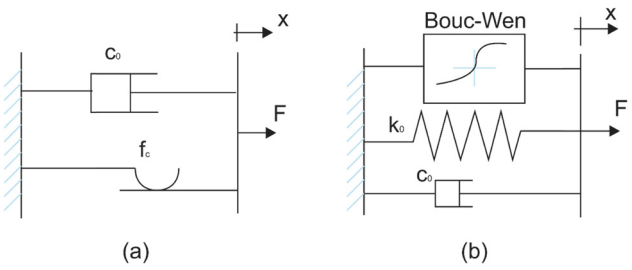

Figure 2: (a) Bingham model and (b) Bouc-Wen model.

Parameter of c_0 is calculated as follows [10]:

$$c_0(V) = 0.179 \times V^2 - 2.048 \times V + 2{,}700. \quad (20)$$

In this research, the input voltage is $V = 15$ volts.

This study aims to select a damper model that can produce the damping force obtained from the SMC strategy. The similarity measure is used as a qualitative measure of a level of confidence and that the damper model can produce the expected damping force.

6 Similarity measures

MR damper design can be started by looking for a similar damper design. The new damper design is then evaluated based on the existing design. By using a similarity measure, the similarity of damper force of the MR damper model and the MR damper to be designed can be explored. Therefore, a functional product design can be obtained.

The similarity measure is usually expressed as a numerical value. The values are higher when the data samples are more alike. It is often expressed as a number between 0 and 1 by conversion: zero means low similarity (the data objects are dissimilar). One means high similarity (the data objects are very similar). Similarity measures are defined by equations (21)–(24) [14]:

$$s(A,\ B) = d((A \cap B\ ), [0]_X) + d((A \cup B), [1]_X), \quad (21)$$

where $d(A, B)$ is the Hamming distance, i.e.,

$$d(A, B) = \frac{1}{n}\sum_{i=1}^{n} |\mu_A(x_i) - \mu_B(x_i)|. \quad (22)$$

A and B are the damping force signal from the Bouc-Wen model and the damping force from the SMC, i.e.,

$$A = \{(x,\ \mu_A(x))|x \in X,\ 0 \le \mu_A(x) \le 1\}, \quad (23)$$

$$B = \{(x,\ \mu_B(x))|x \in X,\ 0 \le \mu_B(x) \le 1\}, \quad (24)$$

where X is the set domain (time) and μ_X is the signal function. A and B are overlapped data.

7 Simulation parameters

Parameters based on ref. [12] are presented in Table 1. Symbols and definitions are explained in Section 2.1 and Figure 1.

8 SMC simulation

The state equation of the semi-active suspension system is expressed with equation (25):

$$\dot{X} = AX + Bh + F, \quad (25)$$

where h is road roughness profile. A is the system matrix and B is the input matrix. System matrix A is expressed as follows:

$$A = \begin{bmatrix} 0 & 0 & 1 & 0 \\ 0 & 0 & 0 & 1 \\ -\frac{k_s}{m_s} & \frac{k_s}{m_s} & \frac{c_s}{m_s} & -\frac{c_s}{m_s} \\ \frac{k_s}{m_u} & -\left(\frac{k_s}{m_u} + \frac{k_t}{m_u}\right) & -\frac{c_s}{m_u} & \frac{c_s}{m_u} \end{bmatrix};$$

$$B = \begin{bmatrix} 0 & 0 & 0 & \frac{k_t}{m_u} \end{bmatrix}^T.$$

F is the control action:

$$F = \begin{bmatrix} 0 & 0 & -\frac{1}{m_s} & \frac{1}{m_u} \end{bmatrix}^T f_d,$$

where $f_d = u_{eq} + u_{sw}$ as shown in equation (3).

9 Result and discussion

The simulation is conducted using Matlab software. The parameters of SMC are presented in Table 2. These values were selected by trial and error and have resulted in slight chattering around the sliding surface in the e vs $\dot{e}$ plane.

Table 1: Parameters of semi-active suspension system [12]

Parameter	Symbol	Values
Sprung mass	m_s	400 kg
Unsprung mass	m_u	40 kg
Suspension stiffness	k_s	2,100 N/m
Suspension damper coefficient	c_s	1,500 N s/m
Tyre stiffness	k_t	150,000 N/m

The purpose of the suspension system is to achieve suspension deflection, y follows the set point y_d fast. Therefore, the suspension performance can be specified by observing the sprung and unsprung deflection and acceleration of mass. In addition, the control action obtained from the controllers should be produced by the MR damper.

10 Sprung mass and unsprung mass response

Vehicle body deflection is expected to be eliminated immediately because this affects the ride comfort of the driver and passengers. The sprung mass deflection and sprung mass acceleration response are shown in Figure 3(a) and (b), respectively. The input is a step function.

Figure 3(a) shows the sprung mass deflection, which implies settling time. While Figure 3(b) shows the sprung mass acceleration associated with ride comfort quality. The SMC controller produces sprung mass acceleration faster than the passive suspension system, resulting in better ride comfort.

Suspension systems work to isolate vibration caused by road roughness, not to transmit to the vehicle body. Suspension is also intended to maintain continuous contact between the tire and road surface to perform road handling. Displacement and acceleration of unsprung mass determine the performance of suspension influenced by the damping force.

Figure 4(a) shows the unsprung mass deflection, which implies settling time, and Figure 4(b) shows the unsprung mass acceleration related to the quality of vehicle handling. Figure 4(b) shows high acceleration at the beginning of step input. It is because the switching action u_{sw} has not yet been computed.

Table 2: SMC parameters

Parameter	Symbol	Value
Sliding variable constant	c	5
Switching control coefficient	k	50
Signum function coefficient	ε	5

11 Damping force to be applied with MR damper

Figure 5(a) shows the damping force generated by the SMC controller. The figure shows that the damping force contains a sudden change in force and chattering. Therefore, the MR should produce this damping force.

In this study, we selected parametric damper MR models: the Bingham model, the Bouc-Wen model, and the Bouc-Wen model with the hyperbolic tangent function to produce the damping force with the state variable input from the controller (displacement and velocity). Each model has MR damper parameters, as shown in Table 3.

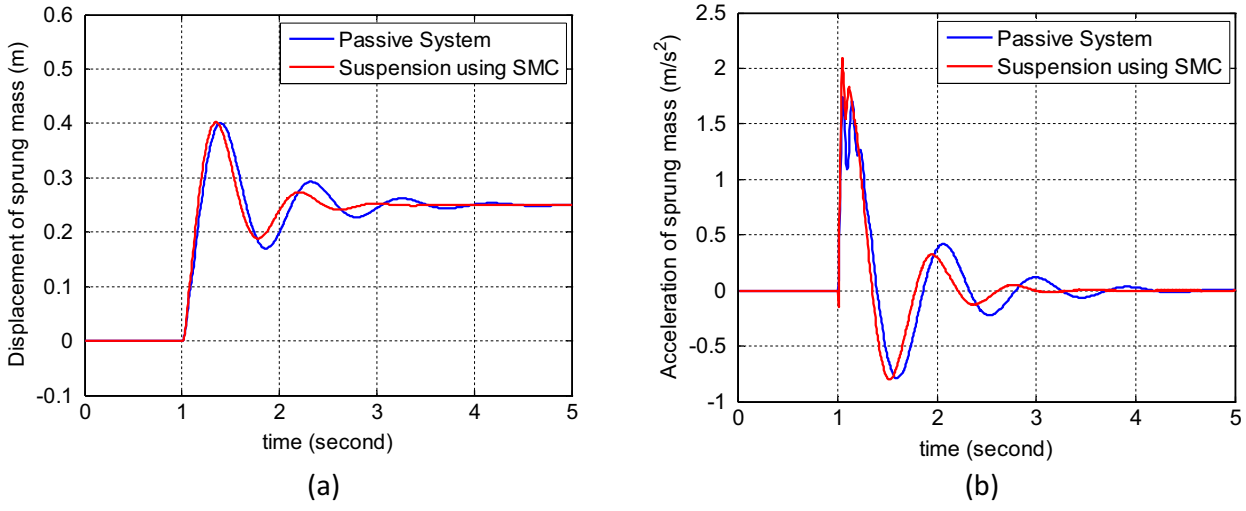

Figure 3: Response of unsprung mass: (a) sprung mass deflection and (b) sprung mass acceleration.

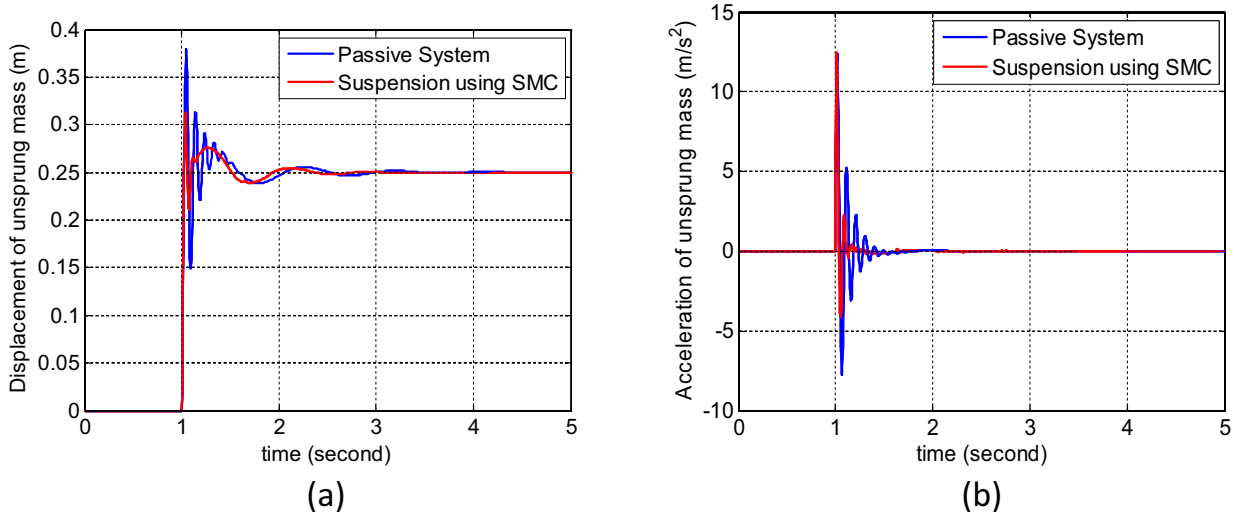

Figure 4: Responses of unsprung mass: (a) unsprung mass deflection and (b) unsprung mass acceleration.

Figure 5(b) shows the damping forces generated by the Bingham model, the Bouc-Wen model, and the Bouc-Wen model with a hyperbolic tangent function. Figure 6 shows that the damping force generated by the MR damper model can track the damping force generated by the SMC controller.

Figure 6 shows that the damping force generated by the Bingham model cannot produce a large damping force at the beginning of the step response. In contrast, the Bouc-Wen model and the Bouc-Wen model with the hyperbolic tangent function can produce a large damping force at the beginning of the step response. The damping force of both Bouc-Wen models shows similar parameter values, as shown in Table 3 (c0, k0, α, β).

Furthermore, the value of similarity measure, $s(A, B)$, is used to assess the similarity of the damping force of the MR model to the damping force generated by the SMC controller. A is the damping force setting of the damper model, and B is the damping force set from the SMC. Similarity measure $s(A, B)$ is calculated using equation (21), where A is the damping force signal set from the Bouc-Wen model and B is the damping force signal set from the SMC. Table 4 presents the value of the similarity measure for the damping force of the MR damper model.

Table 4 shows that the damping force generated by the Bouc-Wen models produces a closer approximation to the damping force from the SMC controller than the Bingham model. The similarity measure is $s = 0.964417$, higher than the Bingham model, which is $s = 0.929852$. Therefore, the Bouc-Wen model can be used as an MR damper model and applied as a component of the semi-active suspension system.

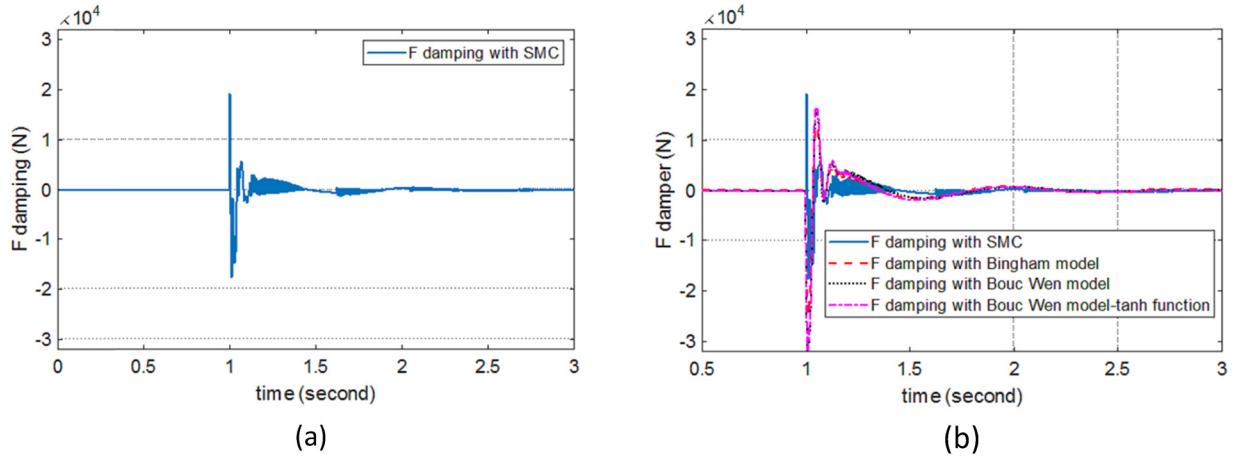

Figure 5: Damping force: (a) damping force: SMC and (b) damping force SMC and models.

Table 3: MR damper model parameter

Bingham model			Bouc Wen model			Bouc Wen model with hyperbolic tangent function		
Parameter	**Value**	**Unit**	**Parameter**	**Value**	**Unit**	**Parameter**	**Value**	**Unit**
c_v	2,000	N s/cm	c_0	Equation (20)	N s/cm	c_0	Equation (20)	N s/cm
F_0	52.83	N	k_0	75	N/cm	k_0	75	N/cm
F_y	100	N/m^2	α	Equation (19)	N/cm	α	0.1	N/cm
			β	1.6	cm^{-2}	β	1.6	cm^{-2}
			γ	1.6	cm^{-2}	δ	0.5	cm^{-2}

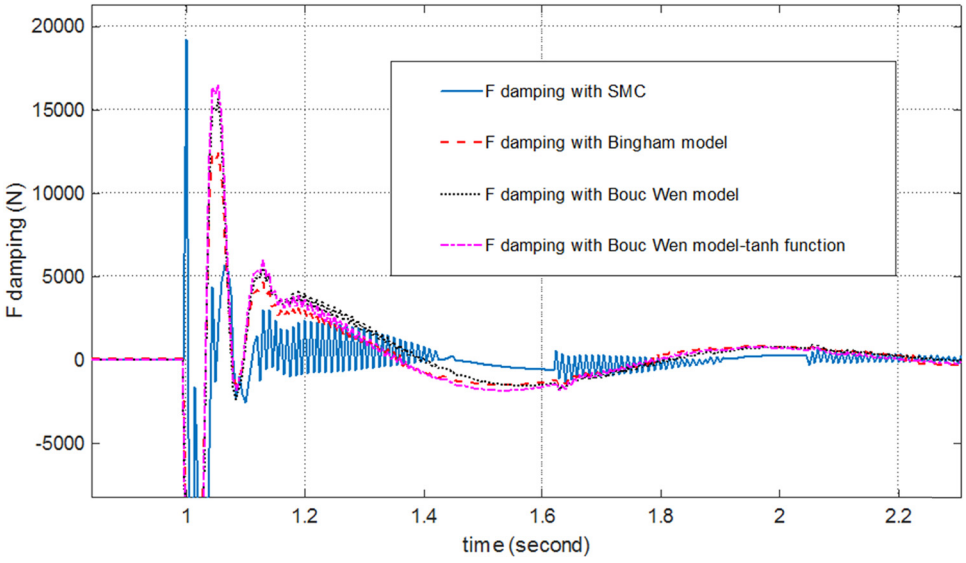

Figure 6: Damper force: SMC and MR damper models (enlarged Figure 5(b)).

Furthermore, to select the MR model that can produce damping forces, the development of the inverse model should be considered. Several parameters of the MR damper are determined as a function of voltage or current, as shown in ref. [20]. The electric current or voltage controls the magnetic field strength and, in turn, changes the properties of the MR fluid, such as viscosity. Furthermore, this study suggests that the Bouc-Wen model with the hyperbolic tangent function is chosen as the MR damper model because the inverse model only requires the variable c_0. Meanwhile, if precise force tracking is needed, the Bouc-Wen model can be used because it uses two variables controlled by an electric voltage.

Table 4: Similarity measure, s (models and SMC damping force)

Model Bingham	Model Bouc Wen	Model Bouc-Wen with hyperbolic tangent function
0.929852	0.964417	0.964417

12 Benchmarking against existing researches

This study aims to design an MR damper for a semi-active suspension system, which is expected to improve ride comfort and road handling. The quarter car model was used, and the SMC control strategy was implemented. Simulation results show that SMC controls can improve that ride quality. Furthermore, the damping force has a small amount of sudden change of force and chattering, so the MR damper should generate it without overloading.

This research had been successfully developed the initial stage of MR damper design, that is, to determine the damper MR model to produce commanded damping force of the SMC controller. The Bouc-Wen damper model is selected. MR damper is a component of a vehicle's semi-active suspension system. Thus, the following research directions for MR damper can be conducted based on the previous study:

- Research develops control strategies to eliminate chattering of SMC. Existing studies include refs. [2,5,15].
- Research to develop the MR damper model. Existing studies include refs. [16–19].
- Research to develop an inverse model of MR damper by using the existing MR damper model. The existing study is ref. [20].

13 Conclusion

This research has successfully determined the MR damper model that can produce the damping force generated by the SMC controller used in vehicle semi-active suspension systems. It is the first step to develop the inverse damper MR model for simulation and experimentation of suspension system using the MR damper.

The Bingham model cannot produce damping forces with sudden changes of force. On the other hand, the Bouc-Wen model and the Bouc-Wen model with the hyperbolic tangent function have a similarity measure of 0.964417 and can produce a sudden force at the beginning of the step response. Furthermore, the Bouc-Wen model was chosen as the MR damper model and for the development of the inverse model, which was applied in the simulation and experimentation of the suspension system with the MR damper.

Acknowledgments: Authors thank to Universitas sebelas maret for the financial support through Hibah Penelitian Grup Riset Non APBN 2023.

Conflict of interest: Authors state no conflict of interest.

References

[1] Yu Y, Royel S, Li J, Li Y, Ha Q. Magnetorheological elastomer base isolator for earthquake response mitigation on building structures-Modeling and second-order sliding mode control. Earthq Struct. 2016;11(6):943–66.

[2] Yao J-L, Zheng J-Q. Semi-active suspension system design for quarter-car model using Model Reference Sliding Mode Control, Conference Paper; January 2007. www.researchgate.net/publication/4353937.

[3] Karaman V, Kayislim KM. Sliding mode control of vehicle suspension system under different road conditions. Int J Eng Sci Appliction. 2017;1(2):72–7.

[4] Ghazaly NM, Makrahy M, Moaaz AO. Sliding mode controller for different road profiles of active suspension system for quarter-car model. Am J Mech Eng. 2019;7(4):151–7.

[5] Kim C, Ro PI. A sliding mode controller for vehicle active suspension system with non-linearities, Proc Instn Mech Engrs vol 212 Part D; 1998.

[6] Rao KD. Modeling, simulation and Control of Semi active suspension system for automobiles under MATLAB simulink using PID controller. Third International Conference on Advances in Control and Optimization of Dynamical System. Kanpur, India: 2014. p. 13–5.

[7] Bai X-X, Wereley NM. Magnetorheological impact seat suspensions for ground vehicle crash mitigation. Active and Passive Smart Structures and Integrated Systems; 2014. doi: 10.1117/12.2045261.

[8] Li W, Zhang X, Du H. Development and simulation evaluation of a magnetorheological elastomer isolator for seat vibration control. J Intell Mater Syst Struct. 2012;23(9):1041–8.

[9] Choi S-B, Han Y-M. Vibration control of electrorheological seat suspension with human body model using sliding mode control. J Sound Vib. 2007;303(2007):391–404.

[10] Rossi A, Orsiini F, Scorza A, Botta F, Belfiore NP, Andrea Sciuto S. 'A review on parametric dynamics models of magnetorheological dampers and their characterization method'. Actuator. 2018;2018(7):16. doi: 10.3390/act702006. www.mdpi.com/journal/actuators.

[11] Li G, Lin H, Ouyang N, Hu G, Xu R, Gu R. Establishment and simulating verification for hyperbolic tangent model of magnetorheological damper. J Phys Conf Ser. 2019;1486(2020):072046. doi: 10.1088/1742-6596/1486/7/072046.

[12] Turakhia TP, Modi MJ. Mathematical modeling and simulation of a simple quarter car vibration model. IJSRD-Int J Sci Res Dev. 2016;3(11):2016. ISSN(online): 2321-0613.

[13] Spencer BF. Phenomenological model of a magnetorheological damper. J Eng Mechanics-March. 1997;123(3):230–38.

[14] Lee S, Shin S. Gait Signal Analysis with similarity measure. Hindawi Publishing Corporation, The Scientific World Journal. 2014;2014:8. Article ID 136018. https://doi.org/10.1155/2014/136018.

[15] Chen Y. Skyhook surface sliding mode control on semi-active vehicle suspension system for ride comfort enhancement. Engineering. 2009;2009(1):1–54.

[16] Nguyen XB, Komatsuzaki T, Iwata Y, Asanuma H. Fuzzy semi-active vibration control of structures using magnetorheological elastomer. Hindawi Shock Vib. 2107;2017. Article ID 2651057.

[17] Wu C, Lin YC, Hsu DS. Performance test and mathematical model simulation of MR damper. The 14 world Conference on Earthquake Engineering. Beijing, China: 2008. p. 12–7.

[18] Shen Y, Golnaraghi MF, Heppler GR. Experimental and modeling of Magnetorheological elastomers. J Intell Mater Syst Struct. 2005;15:27.

[19] Oh J-S, Choi S-B. Ride quality control of a full vehicle suspension system featuring magnetorheological dampers with multiple oriffce holes. Front Mater. 2019;6:8. doi: 10.3389/fmats.2019.0008.

[20] Zhang Z, Huang C, Liu X, Wang X. A novel simplified and high-precision inverse dynamics model for magneto-rheological damper. Appl Mech Mater. 2012;117–119:273. www.scientific.net.